HHS Public Access

Author manuscript

Mol Microbiol. Author manuscript; available in PMC 2019 August 01.

Published in final edited form as:

Mol Microbiol. 2018 August ; 109(3): 401–414. doi:10.1111/mmi.14063.

Novel dual-regulators of *Pseudomonas aeruginosa* are essential for productive biofilms and virulence

Yun Heacock-Kang[1], **Jan Zarzycki-Siek**[1], **Zhenxin Sun**[1], **Kanchana Poonsuk**[2], **Andrew P. Bluhm**[1], **Darlene Cabanas**[1], **Dawson Fogen**[1], **Ian A. McMillan**[1,3], **Rungtip Chuanchuen**[2], and **Tung T. Hoang**[1]

[1]Department of Microbiology, University of Hawaii at Manoa, Honolulu, Hawaii 96822, USA
[2]Department of Veterinary Public Health, Chulalongkorn University, Bangkok 10330, Thailand
[3]Department of Molecular Biosciences and Bioengineering, University of Hawaii at Manoa, Honolulu, Hawaii 96822, USA

Summary

Gene regulation network in *Pseudomonas aeruginosa* is complex. With a relatively large genome (6.2 Mb), there is a significant portion of genes that are proven or predicted to be transcriptional regulators. Many of these regulators have been shown to play important roles in biofilm formation and maintenance. In this study, we present a novel transcriptional regulator, PA1226, which modulates biofilm formation and virulence in *P. aeruginosa*. Mutation in the gene encoding this regulator abolished the ability of *P. aeruginosa* to produce biofilms *in vitro*, without any effect on the planktonic growth. This regulator is also essential for the *in vivo* fitness and pathogenesis in both *Drosophila melanogaster* and BALB/c mouse lung infection models. Transcriptome analysis revealed that PA1226 regulates many essential virulence genes/pathways, including those involved in alginate, pili, and LPS biosynthesis. Genes/operons directly regulated by PA1226 and potential binding sequences were identified via ChIP-seq. Attempts to confirm the binding sequences by electrophoretic mobility shift assay led to the discovery of a co-regulator, PA1413, via co-immunoprecipitation assay. PA1226 and PA1413 were shown to bind collaboratively to the promoter regions of their regulons. A model is proposed, summarizing our finding on this novel dual regulation system.

Graphical Abstract

Correspondence should be addressed to T.T.H. (tongh@hawaii.edu).

Conflict of interest

The authors declare no conflict of interest.

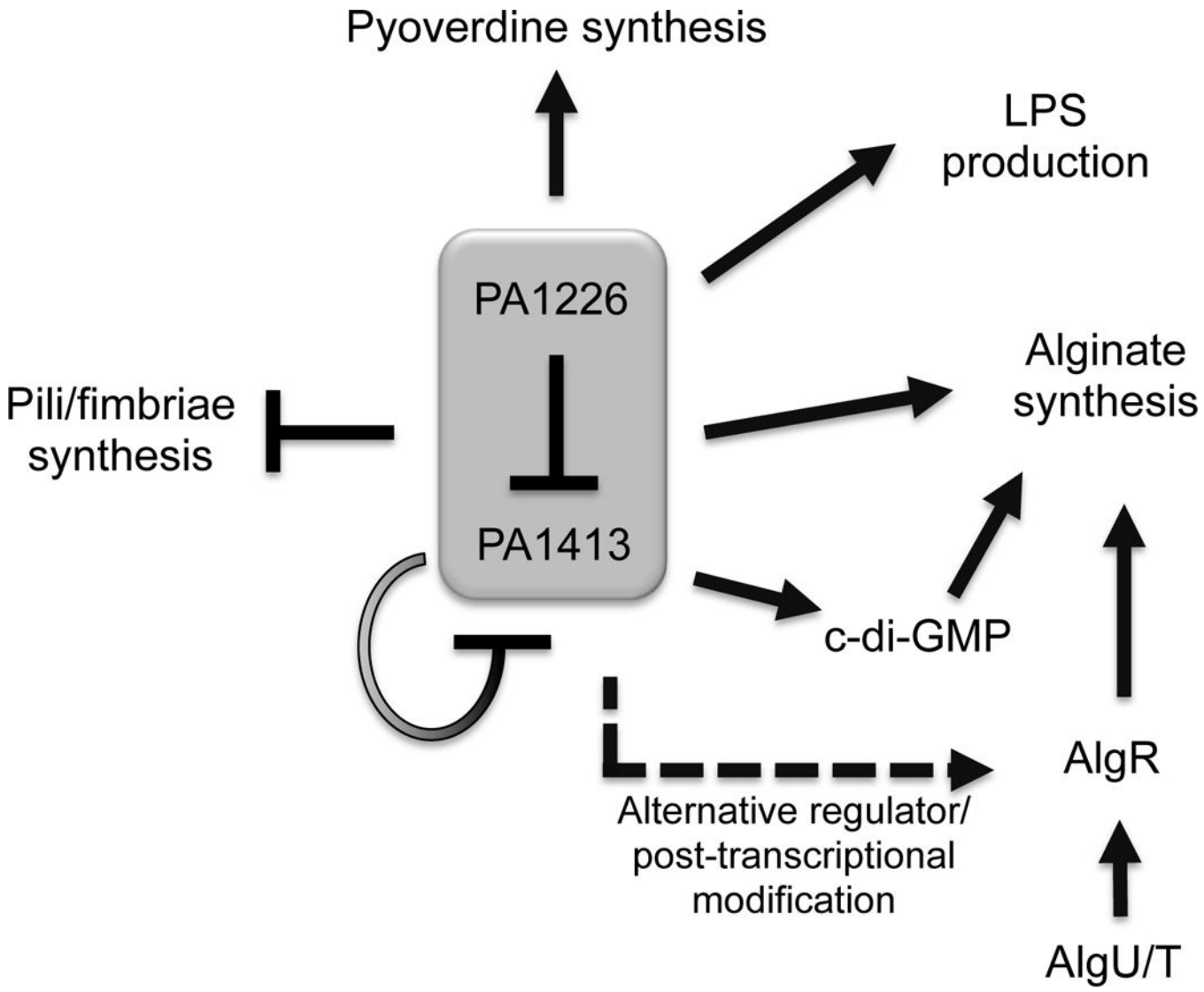

Abbreviated summary

Using our pioneering total transcript amplification of single or a few prokaryotic cells, we have previously uncovered the spatially dependent expressions of thousands of genes in the *Pseudomonas aeruginosa* biofilm architecture. This observation suggests a complex bacterial regulation network controlling bacterial behaviors, which led to the discovery of a novel dual-regulator system presented in this work, PA1226 and PA1413. This dual-regulator system is shown to play essential roles in biofilm formation, *in vivo* fitness and pathogenesis in two animal infection models. Collaboratively, PA1226 and PA1413 modulate the gene expressions of several essential virulence determinants, including alginate, LPS, pyoverdine, and pili/fimbriae biosynthesis operons.

Introduction

Pseudomonas aeruginosa is a saprophytic opportunistic pathogen, exceptionally diverse in its spectrum of human infections. This Gram-negative bacterium causes chronic lung infections in the majority of cystic fibrosis (CF) patients (Govan & Nelson, 1992, Doring, 1997) and is one of the primary causative agents of hospital-acquired pneumonia (Bowton, 1999, Richards *et al.*, 1999, Lode *et al.*, 2000). *P. aeruginosa* produces several virulence factors and has natural resistance to many antimicrobial compounds and the ability to form biofilms in various environments. Additionally, *P. aeruginosa* has a complex network of genes that responds to different conditions, and constantly adapts to environmental changes. With these characteristics, *P. aeruginosa* has been a model organism for the investigation of biofilm (Davies *et al.*, 1998, Singh *et al.*, 2000, O'Loughlin *et al.*, 2013), virulence (Passador *et al.*, 1993, Rahme *et al.*, 1995, Sato *et al.*, 2005, Kang *et al.*, 2009), and quorum sensing (Pearson *et al.*, 1995, De Kievit *et al.*, 2001, Pearson *et al.*, 1997, Pearson *et al.*, 1994). A few valuable vertebrate and invertebrate animal models have been established to study the relationship between *P. aeruginosa* biofilm and pathogenesis, such as BALB/c mouse lung infection model and *Drosophila melanogaster* feeding model (Mulcahy *et al.*, 2011, Hoffmann *et al.*, 2005).

Biofilms represent a lifestyle that allows microorganisms to survive hostile environments and provide a more energy efficient way of obtaining nutrients for growth. Bacteria are capable of forming biofilms on a wide range of surfaces and are relevant in natural, industrial, and clinical settings (Mittelman, 1998, Reed & Kemmerly, 2009, Leaper *et al.*, 2010). Clinically, biofilms are responsible for many persistent and chronic infections attributable to their tolerance to antimicrobial agents and the selection for phenotypic variants that are fit to survive and thrive in infected hosts (Van Acker *et al.*, 2014, Davies, 2003, Mah & O'Toole, 2001). Biofilm formation is a complex process involving environmental signals and a fine-tuned regulation network. During biofilm formation and maturation, the bacteria undergo dynamic shifts in behavior where a large array of genes is differentially regulated (Heacock-Kang *et al.*, 2017, Fazli *et al.*, 2014, Whiteley *et al.*, 2001). This differential regulation of genes is in response to changes in many microenvironmental factors including nutrients, antimicrobial components, as well as signals from neighboring organisms (Heacock-Kang *et al.*, 2017, Fazli *et al.*, 2014, Whiteley *et al.*, 2001). From the initial attachment of planktonic bacteria to a solid surface, through the construction of the micro/macrocolony structure, and finally during maturation of the biofilm, many regulators are responsible for sensing the changes in the microenvironments and controlling the bacterial behaviors in order to achieve a productive biofilm (Heacock-Kang *et al.*, 2017, Fazli *et al.*, 2014). Therefore, gene regulation in the complex biofilm system is essential for our understanding of biofilm formation, maintenance, and dispersion. A better understanding of the genetic and molecular mechanisms of biofilm formation may provide strategies for the control of chronic infections and problems related to biofilm formation.

The molecular structures of *P. aeruginosa* biofilm have been well studied. At least three polysaccharides (Psl, Pel, and alginate) have been identified in *P. aeruginosa* that play important roles in structure maintenance and antibiotic resistance of biofilm (Ma *et al.*, 2009). Additional biofilm components including extracellular DNA, proteins, fimbriae, pili,

and flagellum are also involved in biofilm formation and development (Whitchurch *et al.*, 2002, Mann & Wozniak, 2012). To date, regulation of *P. aeruginosa* biofilm matrix has been described by multiple systems, including quorum sensing (Schuster & Greenberg, 2006), c-di-GMP (Remminghorst & Rehm, 2006, Alm *et al.*, 1996, Hickman & Harwood, 2008), AlgC (Ma *et al.*, 2012), and the AlgZR (Okkotsu *et al.*, 2014) and GacA/GacS (Jimenez *et al.*, 2012) two-component systems. However, our understanding of the *P. aeruginosa* biofilm regulation network is far from comprehensive. Here, we present a new piece of the puzzle, a dual co-regulatory system that modulates the formation of biofilm and virulence in *P. aeruginosa.*

Results and Discussion

Identification of novel transcriptional regulators involved in biofilm formation.

We have recently generated functional genomic data from spatially distinct regions of *P. aeruginosa* biofilm architecture (Heacock-Kang *et al.*, 2017), using our pioneering total transcript amplification of single or a few prokaryotic cells (Kang *et al.*, 2011, Kang *et al.*, 2015). The transcriptomic data have conclusively demonstrated that the expression of thousands of genes is largely dependent on the spatial location in the biofilm architecture. This suggested a complex bacterial regulation network controlling the bacterial behaviors at different locations within the biofilm. We observed the spatial expression patterns of large numbers of genes encoding for hypothetical proteins, many of which are probable transcriptional regulators (Heacock-Kang *et al.*, 2017). We hypothesized that some of these spatially expressed regulators could be important for controlling and, hence, establishing a structurally and functionally mature biofilm. Hundreds of transcriptional regulators are spatially expressed in *P. aeruginosa* biofilm (Heacock-Kang *et al.*, 2017); therefore an initial biofilm formation screen was performed for 42 *P. aeruginosa* mutants, in genes encoding putative regulators that were clearly expressed at spatially defined regions of the biofilm (Fig. S1A). All 42 mutants were obtained from the *P. aeruginosa* Two-Allele Library (Jacobs *et al.*, 2003). Among these 42 regulatory mutants, a mutant strain with an insertional mutation in the regulator PA1226 was shown to have the most significant reduction in biofilm formation via crystal violet assay (Figs. 1A and S1B). Therefore, we chose to focus our efforts on investigating the role PA1226 plays in biofilm formation in this study. This reduced ability to produce biofilm is completely complemented by a single copy of the PA1226 gene via mini-Tn7 insertion (Choi & Schweizer, 2006) into the mutant strain (PA1226 comp in Fig. 1B). Although PA1226 mutant has reduced amount of total biomass relative to wild-type level shown in Fig. 1B, the numbers of bacteria present in the biofilm formed by PA1226 mutant strain is comparable to the wild-type PAO1 and complemented strain (Fig. 1C). The biofilm structures of the PAO1 and PA1226 mutant strains labeled with red fluorescence protein (RFP) were observed under confocal microscopy, and significantly reduced biomass of PA1226 mutant compared to PAO1 is clearly visualized (Fig. 1D). Additionally, this inability in biofilm formation is not resulting from a growth defect, as Figure 1E clearly indicates that PA1226 mutant grow as well as the wild-type and complemented strains *in vitro* in shaking biofilm minimal media.

PA1226 plays an important role in the *Drosophila* and BALB/c pathogenesis models.

The ability of *P. aeruginosa* to form biofilm is one of the key elements for its *in vivo* pathogenesis (Mulcahy *et al.*, 2011, Hoffmann *et al.*, 2005), as biofilm formation is linked to colonization and virulence factor expressions in host. Two infection models, *D. melanogaster* and BALB/c mouse, were utilized to assess the effect of PA1226 on virulence (Mulcahy *et al.*, 2011, Hoffmann *et al.*, 2005). In the fruit fly feeding model, the PA1226 mutant strain was outcompeted in whole fly by the complemented strain (Fig. 2A), and was unable to colonize the crop compared to its complemented strain (Fig. 2B). The inability of PA1226 mutant strain to colonize the fly crop agreed with the link between biofilm formation *in vitro* and attachment/colonization *in vivo*. Additionally, PA1226 mutant strain has reduced virulence shown by a decreased ability in killing fruit flies (Fig. 2C). The reduced *in vivo* fitness of PA1226 mutant strain was also observed in the BALB/c mouse lung infection model (Fig. 2D), further validating that PA1226 plays an important role in biofilm formation as well as *in vivo* pathogenesis. The importance of PA1226 in regulating and virulence both *in vitro* and *in vivo* prompted the identification of pathways that PA1226 controls.

Genes and pathways regulated by PA1226.

The transcriptional regulator PA1226 was shown above to be involved in modulating biofilm production and pathogenesis. To identify the genes/pathways that are directly controlled by PA1226, we carried out ChIP-seq analysis. Using an engineered PAO1 strain harboring a TY-1 tagged PA1226, native DNA fragments that are directly interacting with PA1226 protein were co-precipitated from the clarified bacteria lysates and identified via Illumina next-generation-sequencing (Fig. S2). A total of 38 million high quality reads were obtained and mapped to PAO1 genome, and 10 peaks were determined significant above background (Fig. 3A). These peaks were located in the intergenic regions, upstream of the genes/operons (PA# in Fig. 3A and Table 1) that could be directly regulated by PA1226. Because of the depth of our sequencing (38 million reads) centralizing around the binding sites for PA1226, we were able to use the online software CompleteMOTIFs (Kuttippurathu *et al.*, 2011), to identify the binding motif of PA1226. The binding motif was predicted to be a 14 bp sequence, consisting of semi-conserved 4 bp on each end flanking a random 6 bp spacer (Fig. 3B, $TCTTN_6AAGA$ or $TTCTN_6AGAA$). This motif was conserved among nine out of the 10 sequences, with the exception of PA1413 upstream region containing a 7 bp spacer ($TTCTN_7AGAA$). Among the 10 genes that are predicted to be directly regulated by PA1226, four genes encode for proteins that have known functions: PA2403/*fpvG*, PA3150/*wbpG*, PA3540/*algD*, and PA4550/*fimV*. PA2403/*fpvG* is in an operon that was recently identified to be involved in pyoverdine production (Ganne *et al.*, 2017). PA3150/*wbpG* is the first gene in an operon (PA3150/*wbpG*, PA3149/*wbpH*, and PA3148/*wbpI*), which encodes for LPS biosynthesis proteins (Burrows *et al.*, 1996). PA3540/*algD* encodes for GDP-mannose 6-dehydrogenase (Tatnell *et al.*, 1994), which is the first gene in a nine-gene operon (PA3540-PA3548) responsible for alginate production. PA4550 is predicted to be in an operon for type 4 fimbriae biogenesis (PA4550 to PA4556) (Belete *et al.*, 2008). The other 6 genes are hypothetical/putative genes (3 genes) and probable transcriptional regulators (3 genes). It is worth noting that one of the probable transcriptional regulators, PA1413, was characterized in our recent study (Heacock-Kang *et al.*, 2017), where mutation

in PA1413 caused a defect in biofilm formation and significantly reduced level of intracellular c-di-GMP (Heacock-Kang *et al.*, 2017).

The finding that PA1226 directly regulates three other probable transcriptional regulators led us to further investigate its complex regulation network through microarray analysis. Comparing gene expressions in wild-type PAO1 and PA1226 mutant strains uncovered hundreds of genes indirectly modulated by PA1226 (Tables S1 and S2). All ten directly regulated genes identified via ChIP-seq were present in microarray data, with significant fold-changes (≥2, P <0.05). Collectively, the ChIP-seq and microarray results presented a comprehensive picture of the PA1226 regulation network, and revealed many genes/pathways potentially contributing to biofilm formation and pathogenesis.

Direct interaction of PA1226 and its binding motif.

To validate the binding sequences discovered via ChIP-seq, His-tagged recombinant protein PA1226 was purified using *E. coli* T7 expression system to near homogeneity for electrophoretic mobility shift assay (EMSA). Numerous attempts of EMSA have failed over several months of efforts, using the predicted binding regions upstream of multiple genes regulated by PA1226 (PA1413, *wbpG*, *algD*, PA4203, and *fimU*). To address this hurdle, we replaced the purified His_6-PA1226 with clarified whole cell lysates of PAO1, and successfully detected shifting of the DNA fragments of PA1413 promoter region as an example (Fig. 3C). In contrast, clarified lysate of PA1226 deletion mutant was unable to bind to and shift the DNA fragments (Fig. 3C). Additionally, deletion of the predicted 15 bp binding motif from DNA fragments completely abolished the shift (Fig. 3C, P_{PA1413}-Δmotif). We reasoned that two possibilities could cause this inconsistency using purified protein and clarified lysate: 1) the His-tag affected the conformation or activity of recombinant protein His_6-PA1226; or 2) other proteins/factors in *P. aeruginosa* are necessary for the interaction between PA1226 and DNA. The first possibility was proven unlikely when introduced in *E. coli*, untagged PA1226 did not change the promoter activity of P_{algD}-*lacZ* and P_{wbpG}-*lacZ* (Fig. S3). Therefore, the second scenario is likely that *P. aeruginosa* uses co-regulator(s) to control the binding of PA1226 to the promoter regions of its regulons. To further investigate this hypothesis, we employed the protein co-immunoprecipitation assay in searching for a potential protein partner(s) necessary for PA1226 and DNA interaction (Fig. S4). Two distinct protein bands were observed on an SDS-PAGE gel (Fig. S4) and identified via Ion-Trap LC-MS to be PA1226 and PA1413; PA1413 is one of three probable transcriptional regulators that were directly regulated by PA1226 (Fig. 3A and Table 1).

Armed with this new data, we hypothesized that PA1226 and PA1413 may collaboratively bind to DNA, EMSA was attempted again using a combination of purified His_6-PA1226 and His_6-PA1413. As shown in Fig. 3D, PA1226 and PA1413 together shifted the DNA fragments completely. Conclusively, the interaction of regulator-coregulator-DNA complex was confirmed *in vitro*.

Real-time imaging of PA1226-PA1413-DNA interaction.

Beyond qualitative confirmation of the regulator-coregulator-DNA binding by EMSA, we sought to quantitatively measure such interaction via localized surface plasmon resonance (LSPR). His_6-PA1413 was coupled onto NTA-Ni gold chip, untagged PA1226 and/or DNA containing binding sequences was run through the chip and changes in absorbance were measured. Neither DNA nor PA1226 alone showed any interaction with His_6-PA1413 (Fig. 4A). When mixture of DNA and PA1226 was injected through the chip, concentration dependent interactions were observed (Fig. 4A). At three lower concentrations (33–200 nM of each PA1226 and DNA), DNA and PA1226 completely dissociated from the chip within 10 minutes. When higher concentrations of PA1226 and DNA were used (300 and 600 nM), the initial dissociation was comparable to the lower concentrations (300–380 seconds window); however, stable complex of PA1226-PA1413-DNA subsequently formed and no dissociation was detected after 380 seconds (Fig. 4A). The dissociation constant was determined to be 0.31 μM, using the on-rate (Fig. 4B) and the off-rate for the first 50 seconds (Fig. 4C).

Validation of PA1226/PA1413 binding motifs via DNA footprinting.

ChIP-seq and EMSA results taken together indicated that PA1226 and PA1413 bind to DNA sequences upstream of their regulons. To verify the binding motif predicted by ChIP-seq, DNA footprinting was performed using an automated DNA Analyzer as previously described (Zianni *et al.*, 2006). A DNA fragment upstream of PA1413 (from base −235 to +143 relative to the start codon of PA1413) containing the binding motif was utilized. A *P. aeruginosa* transcriptional regulator PsrA that does not bind to P_{PA1413} was utilized as negative control. DNA traces were observed across the whole length of P_{PA1413} fragment in Fig. 5 upper panels, indicating that PsrA does not interact with and protect the P_{PA1413} fragment from DNase I digestion. In contrast, there are two distinct regions with very little DNA traces detected when purified PA1226 and PA1413 were mixed with P_{PA1413} fragment, suggesting that these regions were bound to and protected by PA1226 and PA1413. The 15 bp sequence predicted to be the binding motif via ChIP-seq was completely protected from DNase I digestion in the presence of PA1226 and PA1413 (underlined and contained within boxed region B in Fig. 5A). Additionally, a nearby 16 bp region, approximately 8 bp upstream of the predicted binding motif, seemed to be partially protected from DNase I fragmentation (boxed region A in Fig. 5A). When DNA footprinting was repeated with this 16 bp deleted from the fragment, a completely different section was protected from DNase I fragmentation (boxed region A in Fig. 5B). This additional protected region is not sequence specific, suggesting that it is potentially involved in facilitating or stabilizing the interaction to the regulators. Since both regulators have helix-turn-helix DNA binding domain, current data are insufficient to distinguish the binding sequences of PA1226 and/or PA1413. Future studies investigating the crystal structures of PA1226 and PA1413 could yield valuable information on the binding sequence specificity of these regulators.

Modulation of the alginate synthesis operon.

Our data clearly indicated that the alginate biosynthesis operon (PA3540-PA3548) was modulated by this PA1226-PA1413 dual-regulation system (Fig. 3, Table 1 and S1). Since

the *alg*-operon and its regulation were extensively studied, we wanted to thoroughly validate our finding that PA1226 and PA1413 are involved in regulation of *alg*-operon. Initially, a qRT-PCR and an alginate assay using 24 h static cultures of PAO1 and PA1226 mutant strains presented contradicting results (Fig. 6A and 6B, 24 h time point). Microarray data indicated that the expression of the alginate synthesis operon (*algD*-*algL*; PA3540-PA3548) was reduced in the PA1226 mutant strain versus wild-type PAO1 strain (Tables 1 and S1). The qRT-PCR strongly agreed with the microarray data, showing that the expression level of *algD* is reduced by approximately 2-fold in the PA1226 mutant when compared to wild-type PAO1 strain (Fig. 6A). However, the alginate assay showed that the culture supernatant of the PA1226 mutant strain contained twice the amount of alginate compared to PAO1 (Fig. 6B). Further tests on cultures at earlier time points (18 h and 21 h) revealed that the extracellular alginate amount did not correlate with the intracellular levels of the *alg*-transcripts (Fig. 6). This is not entirely surprising since the alginate production, accumulating over time, could be lagging behind the RNA level changes, and post-translational modification could also play a role (Fata Moradali *et al.*, 2015, Whitney *et al.*, 2015). Additionally, the changes in expression of the *alg*-operon occurred between 18 and 21 h (Fig. 6A), suggesting possible involvement of a growth phase dependent factor. Since PA1226-PA1413 together acts as a repressor for PA1413, the expression level of PA1413 could be up-regulated in PA1226 mutant strain; this increased level of PA1413 could possibly enhance the alginate production through increased level c-di-GMP, since PA1413 mutant strain was shown to have reduced c-di-GMP levels (Heacock-Kang *et al.*, 2017). On the other hand, the effect of PA1413 mutation on alginate production is straightforward, where PA1413 mutant strain showed both decreased *algD* expression (Fig. 6A) and alginate production (Fig. 6B) compared to wild-type PAO1 at all three time points. Decreased *algD* expression and alginate production were also observed in PA1226+PA1413 double mutant strain (Fig. 6A and 6B). These results suggest a potential additional regulation mechanism of PA1413 on alginate production, independent of PA1226-PA1413 dual-regulation system. Furthermore, when *mucA* mutation was introduced into all strains, similar trends of alginate regulation was observed (Fig. 6C), even though the overall alginate production levels are significantly higher in the mucoid background. This suggests that the regulation mechanism of PA1226 and PA1413 on alginate production is independent of the anti-sigma factor *mucA*.

Model of the dual-regulator system.

Accumulated data presented here provided valuable insights into the novel roles of the dual-regulators' mechanisms in *P. aeruginosa* biofilm formation. We have previously shown that PA1413 was essential for biofilm formation and virulence in *D. melanogaster* feeding model (Heacock-Kang *et al.*, 2017). In this study, we identified that PA1226 and PA1413 collaboratively modulate the biofilm formation and the expression of multiple important virulence factors. Taken together, the data led to the working model of the regulation of pili, LPS, and alginate production by this dual-regulator system (Fig. 7). The dual-regulator PA1226-PA1413 down-regulates gene expression involved in the biosynthesis of pili/fimbriae, while activating genes for the production of pyoverdine, LPS, and alginate. Its mechanisms in repressing of pili/fimbriae biosynthesis as well as activation of pyoverdine and LPS production are relatively simple, through directly interacting with the promoter

regions of *fimU*, *wbpG, and fpvG*, respectively (Fig. 3). In contrast, the modulation of alginate synthesis by PA1226-PA1413 is more complex and involves multiple players. Our data suggested that the dual-regulators control the expression of alginate production through direct binding to *alg*-operon promoter region (Fig. 3), as well as indirectly through c-di-GMP (Heacock-Kang *et al.*, 2017) and possibly a growth phase dependent modulation and/or post-translational modification (Fig. 6). Additionally, the expression of PA1413 was repressed by the dual-regulators (Fig. 3, Table 1 and S2), adding another layer of complexity to this regulatory system. The *P. aeruginosa* biofilm and pathogenesis regulation is a very complex and sophisticated system, and our data definitely support this argument and provides additional insights. There is no doubt that future studies will reveal additional regulatory components for biofilm formation, and our study is one step forward in the right direction.

Experimental Procedures

Bacterial strains, media, and culturing conditions.

E. coli strain EPMax10B-*lacI*^{q}-*pir* was used as a cloning strain. All mutant strains were obtained from the Two-Allele *P. aeruginosa* transposon library (Jacobs *et al.*, 2003), and complementation was done via single copy mini-Tn7 integration as previously described (Choi & Schweizer, 2006) (Heacock-Kang *et al.*, 2017). The *P. aeruginosa* wild-type strain, PAO1, and its derivatives were cultured in Luria-Bertani medium (LB) or biofilm minimal media (Heacock-Kang *et al.*, 2017).

Crystal violet screening, biofilm CFU determination, and confocal microscopy assay.

Static biofilms were cultivated in 96 well plates and assays were performed as previously described (Heacock-Kang *et al.*, 2017). Briefly, all mutant strains, along with wild-type PAO1 strain as control, were first grown overnight in LB broth. Bacteria grown overnight were harvested via centrifugation, washed twice with LB, and diluted 100x into fresh LB. Diluted cultures were inoculated into a 96-well plate. Plates were covered with aluminum foil and incubated without shaking at 30°C for 48 h. Biofilm formed in the well was then washed with 1xPBS and then stained with crystal violet and quantitated following established protocols (Merritt et al., 2005) (Figs. 1B and S1B). For CFU determination in biofilms formed by these strains, biofilms set up identically as the crystal violet assays were washed with 1xPBS, resuspended in 1xPBS+0.2% triton X-100, and enumerated by serial diluting and plating (Fig. 1C). For confocal microscopy, the cultures were set up identically with the exception of using glass bottom 96-well plate for fluorescence detection. At 48 h post incubation, liquid medium containing planktonic bacterial cells of PAO1 or PA1226 mutant was gently pipetted from each well. Biofilm was fixed by adding 4% (w/v) paraformaldehyde and incubated at room temperature for 30 min. After fixation, paraformaldehyde was washed with 1xPBS and the plate was scanned using an Olympus® FV-1000 confocal microscope. Image stacks were obtained under 1000x magnification using Olympus® Fluoview software and processed with ImageJ software (Fig. 1D).

Infection in animal models with biofilm defective mutants.

D. melanogaster and BALB/c mice infection studies were performed as described (Heacock-Kang *et al.*, 2017). Wild-type PAO1, PA1226 mutant, and its complemented strains were used to infect *D. melanogaster* Canton-S strain to investigate their *in vivo* pathogenesis. For easy visualization, pUCP20-*rfp* or pUCP20-*gfp* was introduced into PA1226 mutant and complemented strain, respectively. The *in vivo* competitive index determination, crop dissection for imaging, as well as survival study were performed as previously described (Heacock-Kang *et al.*, 2017). For the *in vivo* competitive index (CI) study, PA1226 mutant and its complemented strain were mixed at a 1:1 ratio and used for infection. PA1226 complemented strain was tagged with gentamycin resistance marker, which is used for determination of the *in vitro* CI ($CFU_{mutant}/CFU_{complement} = CFU_{total\text{-}complement}/CFU_{complement}$). Flies were left to feed on the bacteria mixture for 2 days before harvesting. Two control experiments were performed: two strains of wild-type PAO1 tagged with either tetracycline resistance and RFP marker or gentamycin resistance and GFP marker were mixed at 1:1 ratio and used for infection; additionally, *in vitro* CI ($CFU_{mutant}/CFU_{complement}$) was determined by culturing PA1226 mutant and complemented strains mixed 1:1 in LB medium, and grown for 2 days. For survival study, three groups of ten flies were used for each individual bacterial strain and monitored for 14 days.

In vivo competition was also performed in BALB/c mice. All animal experiments were approved by the University of Hawaii Institutional Animal Care and Use Committee (protocol No. 06–023), and performed in compliance with the National Institutes of Health Guide for the Care and Use of Laboratory Animals. Six to eight week old male BALB/c mice from Charles River Laboratories were used for the study. *In vivo* competition study was performed as previously described (Heacock-Kang *et al.*, 2017). Prior to intubation, the mice were anesthetized by intraperitoneal injection of 100 mg ketamine and 10 mg xylazine per kg of body weight. Thirty milliliter of the mutant/complemented strain mixture (3×10^7 CFU each) resuspended in purified bacteria-free alginate (Hoffmann et al., 2005) was inoculated intratracheally into BALB/c mice lungs using the BioLITE® Intubation System (Braintree Scientific). A group of five mice was used for the mutant/complemented competition. An additional group of three mice was used for the control competition using 1:1 mixture of two PAO1 strains tagged with gentamycin and tetracycline resistance markers, respectively. Three mice were inoculated with 1xPBS as intratracheal instillation procedure control. At 24 h post inoculation, mice were humanely euthanized and lungs were harvested. Both lungs from each mouse were homogenized in 5 ml total volume of sterile 1xPBS in a Stomacher® 80 Biomaster tissue processor, bacteria loads were quantified, and *in vivo* CI were determined as described above for *in vivo* competition in fruit flies.

Microarray analysis and qRT-PCR validation.

Microarray was performed on PA1226 mutant strain, using PAO1 strain as wild-type control. Static cultures were grown at 37°C for 24 h. RNA isolation and microarray analysis was performed as described elsewhere (Kang *et al.*, 2008, Heacock-Kang *et al.*, 2017). The same RNA samples were used for qRT-PCR validation, using three housekeeping genes (PA1769, PA1795, and PA1805) as controls, as previously described (Kang *et al.*, 2008).

Alginate Assay.

Static biofilm cultures of PAO1 and various mutant strains used in Fig. 6 were grown at 37°C, and alginate purification and measurement was carried out as previously described (Son *et al.*, 2007).

ChIP-seq.

A translational fusion of TY1-tag at the N-terminus of PA1226 gene was constructed by a three-fragment ligation. Vector pUCP20TQ was first constructed by introducing *oriT* and *lacIQ* genes into pUCP20 (West *et al.*, 1994). A PAGE-purified oligo containing three concatemers of the TY1 tag was used as template to PCR-amplify 3xTY1 tag. PA1226 was amplified from PAO1 chromosomal DNA. The amplified 3xTY1 tag was digested with *Eco*RI and *Nde*I, and the amplified PA1226 was digested with *Nde*I and *Hind*III. Both digested fragments were cloned into pUCP20TQ cut with *Eco*RI and *Hind*III. The 3xTY1 tag in the resulting fusion vector and the junction of the fusion were confirmed by sequencing. The fusion vector pUCP20TQ-3xTY1-PA1226 was conjugated into PAO1-PA1226::Tet^r-*lacZ* mutant obtained from the *P. aeruginosa* two-allele transposon mutant library (Jacobs *et al.*, 2003).

P. aeruginosa wild-type PAO1 strain and PA1226 mutant strain containing pUCP20TQ-3xTY1-PA1226 were grown in 2 ml of LB overnight. Cells were diluted 100x into 3 ml of LB medium with 0.25 mM IPTG for induction and grown at 37°C for 24 h without shaking. One ml aliquots were harvested and cell pellets were resuspended and cross-linked by the addition of PFA to a final concentration of 4% and incubation at room temperature for 15 min with gentle mixing. Cross-linking was quenched by addition of glycine to a final concentration of 125 mM (0.75 M stock). Cells were harvested and washed twice with Tris-buffered saline (20 mM Tris-Cl pH 7.5, 150 mM NaCl), and resuspended in 50 µl Immunoprecipitation (IP) buffer (20 mM Tris-Cl pH 7.5, 150 mM NaCl, 2 mM EDTA, 1% Triton X-100, 0.1% SDS, and protease inhibitor cocktail (Roche®)). Lysozyme was added to a final concentration of 1 mg/ml, sufficient lysis was achieved by freezing and thawing 2–3 times. Samples were spun down and supernatants were diluted in nebulization buffer (TE buffer pH8.0 with 10% glycerol). DNA was sheared to an average size of 100–500 bp (majority 200–400 ideally) in a Roche® nebulizer. Fragmented DNA complex containing the TY-1 tagged regulator protein was enriched using TY1 mouse monoclonal antibody and DiaMag® anti-mouse IgG-coated magnetic beads (Diagenode®) following established protocol (Tiwari & Baylin, 2009). Enriched DNA-regulator complex was reverse crosslinked overnight at 65 °C and purified through phenol/chloroform extraction and sodium acetate/isopropanol precipitation. Purified DNA fragments were used as template for library construction according to Illumina ChIP-seq sample preparation protocol and sequenced at TUCF Genomics at Tufts University School of Medicine.

Co-immunoprecipitation assay.

The co-immunoprecipitation assay was performed by using the same PAO1 strain with the 3xTY1-tagged PA1226. Supernatant that contain the DNA-regulator-co-regulator complex were obtained the same way as described above for ChIP-seq. Complex containing the TY-1 tagged regulator protein was enriched using TY1 mouse monoclonal antibody and DiaMag

protein A-coated magnetic beads as aforementioned. Enriched DNA-regulator-co-regulator complex was reverse crosslinked overnight at 65°C and ran on a 10% SDS-PAGE. Bands visible on the SDS-PAGE were extracted and identified by LC Ion-Trap MS/MS at the Proteomics Core Facility at University of Hawaii at Manoa.

Electrophoretic mobility shift assay (EMSA).

EMSA using purified proteins or alternatively *P. aeruginosa* clarified lysate was performed as previously described (Kang *et al.*, 2008). His_6-tagged recombinant proteins were purified as previously described (Kang *et al.*, 2008). Clarified lysates of wild-type PAO1 and derived strains were obtained by first growing cultures in LB overnight. Overnight cultures were then diluted 100x in fresh LB and grown to log-phase. Bacterial cells were harvested, washed twice with 20 mM Tris-Cl pH 7.9, and resuspended in 20 mM Tris-Cl pH7.9, 0.5 M NaCl, 10 mM EDTA, 20 μg/ml lysozyme, and 1 mM DTT. Resuspended cultures were frozen and thawed 2–3 times for complete lysis, and clarified lysates were obtained by centrifugation at 16,000 g at 4°C for 30 min. Amounts of the total protein in the clarified lysates were estimated by Bradford protein assay.

Kinetics measurements using localized surface plasmon resonance (LSPR).

LSPR was performed using an NTA-gold sensor chip on a Nicoya OpenSPR™, following manufacturer instructions. For studying the binding interaction of the complex, purified His_6-PA1413 was first covalently immobilized to an NTA sensor in a non-random orientation using the capture coupling method (Kimple *et al.*, 2010). Untagged PA1226 was purified using expression vector pTYB1 as previously described (Chong *et al.*, 1997). Binding interactions of Untagged PA1226 and/or DNA containing binding sequences to the immobilized ligand on the biosensor was performed under the following conditions. Association measurements were obtained by injecting solutions of purified Untagged PA1226 and DNA containing binding sequences at various concentrations (33 nM, 100 nM, 200 nM, 300 nM, and 600 nM) in HBS buffer (20 mM HEPES, 150 mM NaCl, pH 7.0) and measuring the increase in signal for 300 seconds. Dissociation measurements were obtained by injecting fresh solution of HBS buffer and measuring the decrease in signals for 660 seconds.

DNA Footprinting.

DNA Footprinting was performed with an automated DNA Analyzer as previously described (Zianni *et al.*, 2006). The pUC18 vectors containing the predicted regulator binding sequences were used as a template to generate the ~400 bp probes. The probe was generated by PCR with HPLC purified primers Footprint-up-FAM (5′-(6-FAM)-ACGCCGAAGGCTTCCTCCAAG-3′) and Footprint-down (5′-GTCCTGCAACTCGGCCGGTAT-3′) from Integrated DNA Technologies, Inc. PA1226 and PA1413 proteins were incubated with 500 ng of fluorescently labeled probe for 10 min at room temperature in EMSA buffer (Kang *et al.*, 2008). After this, DNase I was added to the reaction mixture to a final volume of 50 μL and incubated for 20 min at 37°C. Control digestions with the probe were performed in the presence of control regulator protein PsrA. The DNA fragments were purified with the QIAquick PCR Purification kit (Qiagen) and eluted in 40 μL H_2O to

eliminate salts that can interfere with capillary electrophoresis. Digested DNA was then analyzed on the 3730 DNA Analyzer using a G5 dye set.

Data set availability.

The datasets generated in this publication have been deposited in NCBI's Gene Expression Omnibus (Edgar *et al.*, 2002) and are accessible through GEO Series accession number GSE107640.

Supplementary Material

Refer to Web version on PubMed Central for supplementary material.

Acknowledgements

This project was supported by the US National Institutes of Health (NIH)/National Institute of General Medical Sciences (NIGMS) grant number R01GM103580 and in part by US National Institutes of Health (NIH)/National Institute of Allergy and Infectious Diseases (NIAID) grant number R21AI123913. *P. aeruginosa* DNA arrays were obtained through NIAID's Pathogen Functional Genomics Resource Center, managed and funded by the Division of Microbiology and Infectious Diseases, NIAID, NIH, DHHS, and operated by the J. Craig Venter Institute. We would like to thank Allexa Dow for her assistance on the LSPR experimental setup and Dr. Sladjana Prisic for the use of her plasmon resonance instrument.

References

Alm RA, Bodero AJ, Free PD & Mattick JS, (1996) Identification of a novel gene, *pilZ*, essential for type 4 fimbrial biogenesis in *Pseudomonas aeruginosa*. J Bacteriol 178: 46–53. [PubMed: 8550441]

Belete B, Lu H & Wozniak DJ, (2008) *Pseudomonas aeruginosa* AlgR regulates type IV pilus biosynthesis by activating transcription of the *fimU-pilVWXY1Y2E* operon. J Bacteriol 190: 2023–2030. [PubMed: 18178737]

Bowton DL, (1999) Nosocomial pneumonia in the ICU-year 2000 and beyond. Chest 115: 28S–33S. [PubMed: 10084457]

Burrows LL, Charter DF & Lam JS, (1996) Molecular characterization of the *Pseudomonas aeruginosa* serotype O5 (PAO1) B-band lipopolysaccharide gene cluster. Mol Microbiol 22: 481–495. [PubMed: 8939432]

Choi KH & Schweizer HP, (2006) mini-Tn7 insertion in bacteria with single *attTn7* sites: example *Pseudomonas aeruginosa*. Nat Protoc 1: 153–161. [PubMed: 17406227]

Chong S, Mersha FB, Comb DG, Scott ME, Landry D, Vence LM, Perler FB, Benner J, Kucera RB, Hirvonen CA, Pelletier JJ, Paulus H & Xu MQ, (1997) Single-column purification of free recombinant proteins using a self-cleavable affinity tag derived from a protein splicing element. Gene 192: 271–281. [PubMed: 9224900]

Davies D, (2003) Understanding biofilm resistance to antibacterial agents. Nature reviews. Drug discovery 2: 114–122. [PubMed: 12563302]

Davies DG, Parsek MR, Pearson JP, Iglewski BH, Costerton JW & Greenberg EP, (1998) The involvement of cell-to-cell signals in the development of a bacterial biofilm. Science 280: 295–298. [PubMed: 9535661]

De Kievit TR, Gillis R, Marx S, Brown C & Iglewski BH, (2001) Quorum-sensing genes in *Pseudomonas aeruginosa* biofilms: their role and expression patterns. Applied and Environmental Microbiology 67: 1865–1873. [PubMed: 11282644]

Doring G, (1997) Cystic fibrosis respiratory infections: interactions between bacteria and host defense. Monaldi Arch. Chest Dis. 52: 363–366. [PubMed: 9401367]

Edgar R, Domrachev M & Lash AE, (2002) Gene Expression Omnibus: NCBI gene expression and hybridization array data repository. Nucleic Acids Res 30: 207–210. [PubMed: 11752295]

Fata Moradali M, Donati I, Sims IM, Ghods S & Rehm BH, (2015) Alginate polymerization and modification are linked in *Pseudomonas aeruginosa*. mBio 6: e00453–00415. [PubMed: 25968647]

Fazli M, Almblad H, Rybtke ML, Givskov M, Eberl L & Tolker-Nielsen T, (2014) Regulation of biofilm formation in *Pseudomonas* and *Burkholderia* species. Environmental microbiology 16: 1961–1981. [PubMed: 24592823]

Ganne G, Brillet K, Basta B, Roche B, Hoegy F, Gasser V & Schalk IJ, (2017) Iron release from the siderophore pyoverdine in *Pseudomonas aeruginosa* involves three new actors: FpvC, FpvG, and FpvH. ACS chemical biology 12: 1056–1065. [PubMed: 28192658]

Govan JR & Nelson JW, (1992) Microbiology of lung infection in cystic fibrosis. Br. Med. Bull. 48: 912–930. [PubMed: 1281036]

Heacock-Kang Y, Sun Z, Zarzycki-Siek J, McMillan IA, Norris MH, Bluhm AP, Cabanas D, Fogen D, Vo H, Donachie SP, Borlee BR, Sibley CD, Lewenza S, Schurr MJ, Schweizer HP & Hoang TT, (2017) Spatial transcriptomes within the *Pseudomonas aeruginosa* biofilm architecture. Mol Microbiol 106: 976–985. [PubMed: 29030956]

Hickman JW & Harwood CS, (2008) Identification of FleQ from *Pseudomonas aeruginosa* as a c-di-GMP-responsive transcription factor. Mol Microbiol 69: 376–389. [PubMed: 18485075]

Hoffmann N, Rasmussen TB, Jensen PO, Stub C, Hentzer M, Molin S, Ciofu O, Givskov M, Johansen HK & Hoiby N, (2005) Novel mouse model of chronic *Pseudomonas aeruginosa* lung infection mimicking cystic fibrosis. Infect. Immun. 73: 2504–2514. [PubMed: 15784597]

Jacobs MA, Alwood A, Thaipisuttikul I, Spencer D, Haugen E, Ernst S, Will O, Kaul R, Raymond C, Levy R, Chun-Rong L, Guenthner D, Bovee D, Olson MV & Manoil C, (2003) Comprehensive transposon mutant library of *Pseudomonas aeruginosa*. Proc Natl Acad Sci 100: 14339–14344. [PubMed: 14617778]

Jimenez PN, Koch G, Thompson JA, Xavier KB, Cool RH & Quax WJ, (2012) The multiple signaling systems regulating virulence in *Pseudomonas aeruginosa*. Microbiology and molecular biology reviews : MM*BR* 76: 46–65. [PubMed: 22390972]

Kang Y, Lunin VV, Skarina T, Savchenko A, Schurr MJ & Hoang TT, (2009) The long-chain fatty acid sensor, PsrA, modulates the expression of *rpoS* and the type III secretion *exsCEBA* operon in *Pseudomonas aeruginosa*. Mol Microbiol 73: 120–136. [PubMed: 19508282]

Kang Y, McMillan I, Norris MH & Hoang TT, (2015) Single prokaryotic cell isolation and total transcript amplification protocol for transcriptomic analysis. Nat Protoc 10: 974–984. [PubMed: 26042386]

Kang Y, Nguyen DT, Son MS & Hoang TT, (2008) The *Pseudomonas aeruginosa* PsrA responds to long-chain fatty acid signals to regulate the *fadBA5* b-oxidation operon. Microbiology 154: 1584–1598. [PubMed: 18524913]

Kang Y, Norris MH, Zarzycki-Siek J, Nierman WC, Donachie SP & Hoang TT, (2011) Transcript amplification from single bacterium for transcriptome analysis. Genome Res 21: 925–935. [PubMed: 21536723]

Kimple AJ, Muller RE, Siderovski DP & Willard FS, (2010) A capture coupling method for the covalent immobilization of hexahistidine tagged proteins for surface plasmon resonance. Methods in molecular biology 627: 91–100. [PubMed: 20217615]

Kuttippurathu L, Hsing M, Liu Y, Schmidt B, Maskell DL, Lee K, He A, Pu WT & Kong SW, (2011) CompleteMOTIFs: DNA motif discovery platform for transcription factor binding experiments. Bioinformatics 27: 715–717. [PubMed: 21183585]

Leaper D, McBain AJ, Kramer A, Assadian O, Sanchez JL, Lumio J & Kiernan M, (2010) Healthcare associated infection: novel strategies and antimicrobial implants to prevent surgical site infection. Annals of the Royal College of Surgeons of England 92: 453–458. [PubMed: 20819330]

Lode H, Raffenberg M, Erbes R, Geerdes-Fenge H & Mauch H, (2000) Nosocomial pneumonia: epidemiology, pathogenesis, diagnosis, treatment and prevention. Curr. Opin. Infect. Dis. 13: 377–384. [PubMed: 11964806]

Ma L, Conover M, Lu H, Parsek MR, Bayles K & Wozniak DJ, (2009) Assembly and development of the *Pseudomonas aeruginosa* biofilm matrix. PLoS Pathog 5: e1000354. [PubMed: 19325879]

Ma L, Wang J, Wang S, Anderson EM, Lam JS, Parsek MR & Wozniak DJ, (2012) Synthesis of multiple *Pseudomonas aeruginosa* biofilm matrix exopolysaccharides is post-transcriptionally regulated. Environmental microbiology 14: 1995–2005. [PubMed: 22513190]

Mah T-FC & O'Toole GA, (2001) Mechanisms of biofilm resistance to antimicrobial agents. Trends Microbiol. 9: 34–39. [PubMed: 11166241]

Mann EE & Wozniak DJ, (2012) *Pseudomonas* biofilm matrix composition and niche biology. FEMS microbiology reviews 36: 893–916. [PubMed: 22212072]

Mittelman MW, (1998) Structure and functional characteristics of bacterial biofilms in fluid processing operations. Journal of dairy science 81: 2760–2764. [PubMed: 9812281]

Mulcahy H, Sibley CD, Surette MG & Lewenza S, (2011) *Drosophila melanogaster* as an animal model for the study of *Pseudomonas aeruginosa* biofilm infections *in vivo*. PLoS Pathog 7: e1002299. [PubMed: 21998591]

O'Loughlin CT, Miller LC, Siryaporn A, Drescher K, Semmelhack MF & Bassler BL, (2013) A quorum-sensing inhibitor blocks *Pseudomonas aeruginosa* virulence and biofilm formation. Proceedings of the National Academy of Sciences 110: 17981–17986.

Okkotsu Y, Little AS & Schurr MJ, (2014) The *Pseudomonas aeruginosa* AlgZR two-component system coordinates multiple phenotypes. Frontiers in cellular and infection microbiology 4: 82. [PubMed: 24999454]

Passador L, Cook JM, Gambello MJ, Rust L & Iglewski BH, (1993) Expression of *Pseudomonas aeruginosa* virulence genes requires cell-to-cell communication. Science 260: 1127–1130. [PubMed: 8493556]

Pearson J, Gray K, Passador L, Tucker K, Eberhard A, Iglewski B & Greenberg E, (1994) Structure of the autoinducer required for expression of *Pseudomonas aeruginosa* virulence genes. Proc. Natl. Acad. Sci. USA 91: 197–201. [PubMed: 8278364]

Pearson J, Passador L, Iglewski B & Greenberg E, (1995) A second *N*-acylhomoserine lactone signal produced by *Pseudomonas aeruginosa*. Proc. Natl. Acad. Sci. USA 92: 1490–1494. [PubMed: 7878006]

Pearson JP, Pesci EC & Iglewski BH, (1997) Roles of *Pseudomonas aeruginosa las* and *rhl* quorum-sensing systems in control of elastase and rhamnolipid biosynthesis genes. J. Bacteriol. 179: 5756–5767. [PubMed: 9294432]

Rahme LG, Stevens EJ, Wolfort SF, Shao J, Tompkins RG & Ausubel FM, (1995) Common virulence factors for bacterial pathogenicity in plants and animals. Science 268: 1899–1902. [PubMed: 7604262]

Reed D & Kemmerly SA, (2009) Infection control and prevention: a review of hospital-acquired infections and the economic implications. The Ochsner journal 9: 27–31. [PubMed: 21603406]

Remminghorst U & Rehm BH, (2006) Alg44, a unique protein required for alginate biosynthesis in *Pseudomonas aeruginosa*. FEBS letters 580: 3883–3888. [PubMed: 16797016]

Richards MJ, Edwards JR, Culver DH & Gaynes RP, (1999) Nosocomial infections in medical intensive care units in the United States. Crit. Care Med. 27: 887–892. [PubMed: 10362409]

Sato H, Feix JB, Hillard CJ & Frank DW, (2005) Characterization of phospholipase activity of the *Pseudomonas aeruginosa* type III cytotoxin, ExoU. J. Bacteriol. 187: 1192–1195. [PubMed: 15659695]

Schuster M & Greenberg EP, (2006) A network of networks: quorum-sensing gene regulation in *Pseudomonas aeruginosa*. International journal of medical microbiology : IJMM 296: 73–81.

Singh PK, Schaefer AL, Parsek MR, Moninger TO, Welsh MJ & Greenberg EP, (2000) Quorum-sensing signals indicate that cystic fibrosis lungs are infected with bacterial biofilms. Nature 407: 762–764. [PubMed: 11048725]

Son MS, Matthews WJJ, Kang Y, Nguyen DT & Hoang TT, (2007) *In vivo* evidence of *Pseudomonas aeruginosa* nutrient acquisition and pathogenesis in the lungs of cystic fibrosis patients. Infect. Immun. 75: 5313–5324. [PubMed: 17724070]

Tatnell PJ, Russell NJ & Gacesa P, (1994) GDP-mannose dehydrogenase is the key regulatory enzyme in alginate biosynthesis in *Pseudomonas aeruginosa*: evidence from metabolite studies. Microbiology 140 **(**Pt 7**)**: 1745–1754. [PubMed: 7521247] **()**

Tiwari VK & Baylin SB, (2009) Combined 3C-ChIP-Cloning (6C) assay: a tool to unravel protein-mediated genome architecture. Cold Spring Harbor protocols 2009.

Van Acker H, Van Dijck P & Coenye T, (2014) Molecular mechanisms of antimicrobial tolerance and resistance in bacterial and fungal biofilms. Trends in microbiology 22: 326–333. [PubMed: 24598086]

West SEH, Schweizer HP, Dall C, Sample AK & Runyen-Janecky LJ, (1994) Construction of improved *Escherichia-Pseudomonas* shuttle vectors derived from pUC18/19 and the sequence of the region required for their replication in *Pseudomonas aeruginosa*. Gene 128: 81–86.

Whitchurch CB, Tolker-Nielsen T, Ragas PC & Mattick JS, (2002) Extracellular DNA required for bacterial biofilm formation. Science 295: 1487. [PubMed: 11859186]

Whiteley M, Bangera MG, Bumgarner RE, Parsek MR, Teitzel GM, Lory S & Greenberg EP, (2001) Gene expression in *Pseudomonas aeruginosa* biofilms. Nature 413: 860–864. [PubMed: 11677611]

Whitney JC, Whitfield GB, Marmont LS, Yip P, Neculai AM, Lobsanov YD, Robinson H, Ohman DE & Howell PL, (2015) Dimeric c-di-GMP is required for post-translational regulation of alginate production in *Pseudomonas aeruginosa*. The Journal of biological chemistry 290: 12451–12462. [PubMed: 25817996]

Zianni M, Tessanne K, Merighi M, Laguna R & Tabita FR, (2006) Identification of the DNA bases of a DNase I footprint by the use of dye primer sequencing on an automated capillary DNA analysis instrument. Journal of Biomolecular Techniques : JBT 17: 103–113. [PubMed: 16741237]

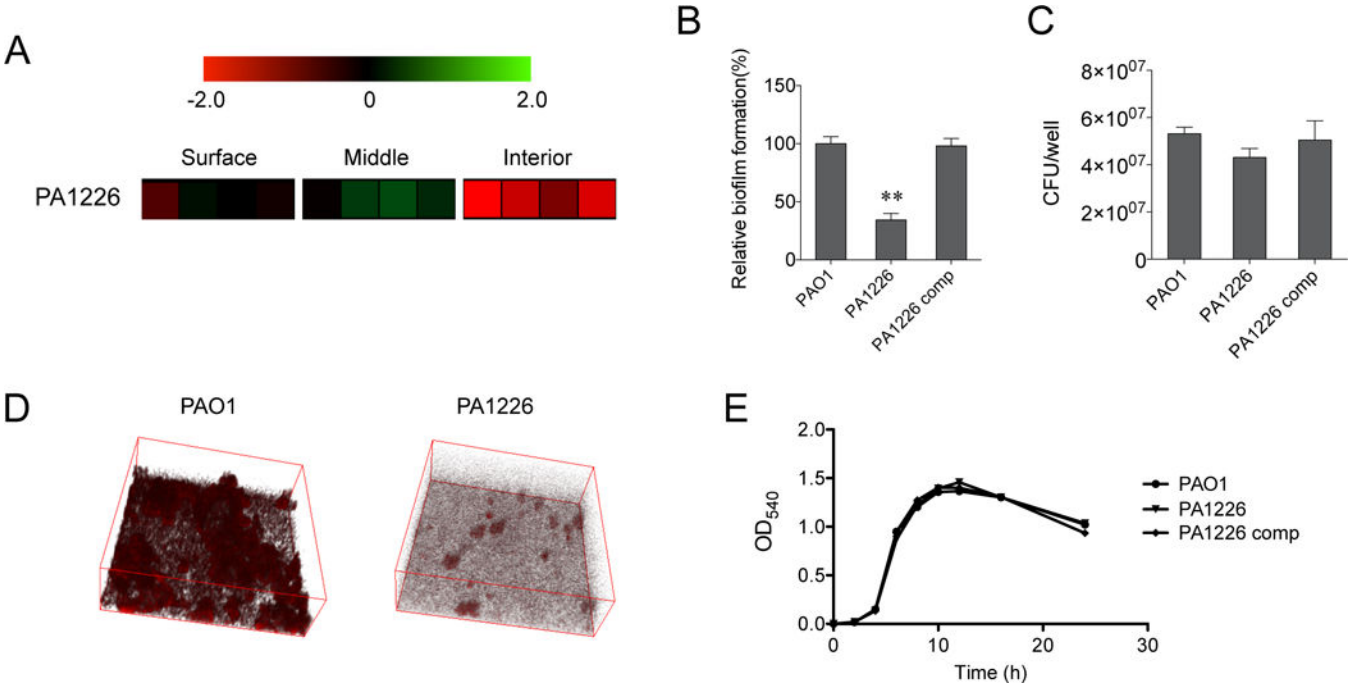

Figure 1.

Identification of regulator PA1226 essential for biofilm formation. (A) PA1226 is differentially expressed in three locations within the biofilm structure from previously published data (Heacock-Kang *et al.*, 2017). Gene expression fold-changes are shown with a red-black-green double color gradient. (B) The mutant of PA1226 has significantly reduced biofilm formation via crystal violet assay (**, $P < 0.005$ based on unpaired *t*-test) compared to wild-type strain PAO1 and the complemented PA1226 strain (PA1226 comp). (C) Numbers of bacteria present in the biofilm structure are comparable between PAO1 wild-type, PA1226 mutant, and its complemented strain. (D) Structural defects in biofilm were visualized under confocal microscopy. (E) Mutation in PA1226 has no affect on planktonic growth.

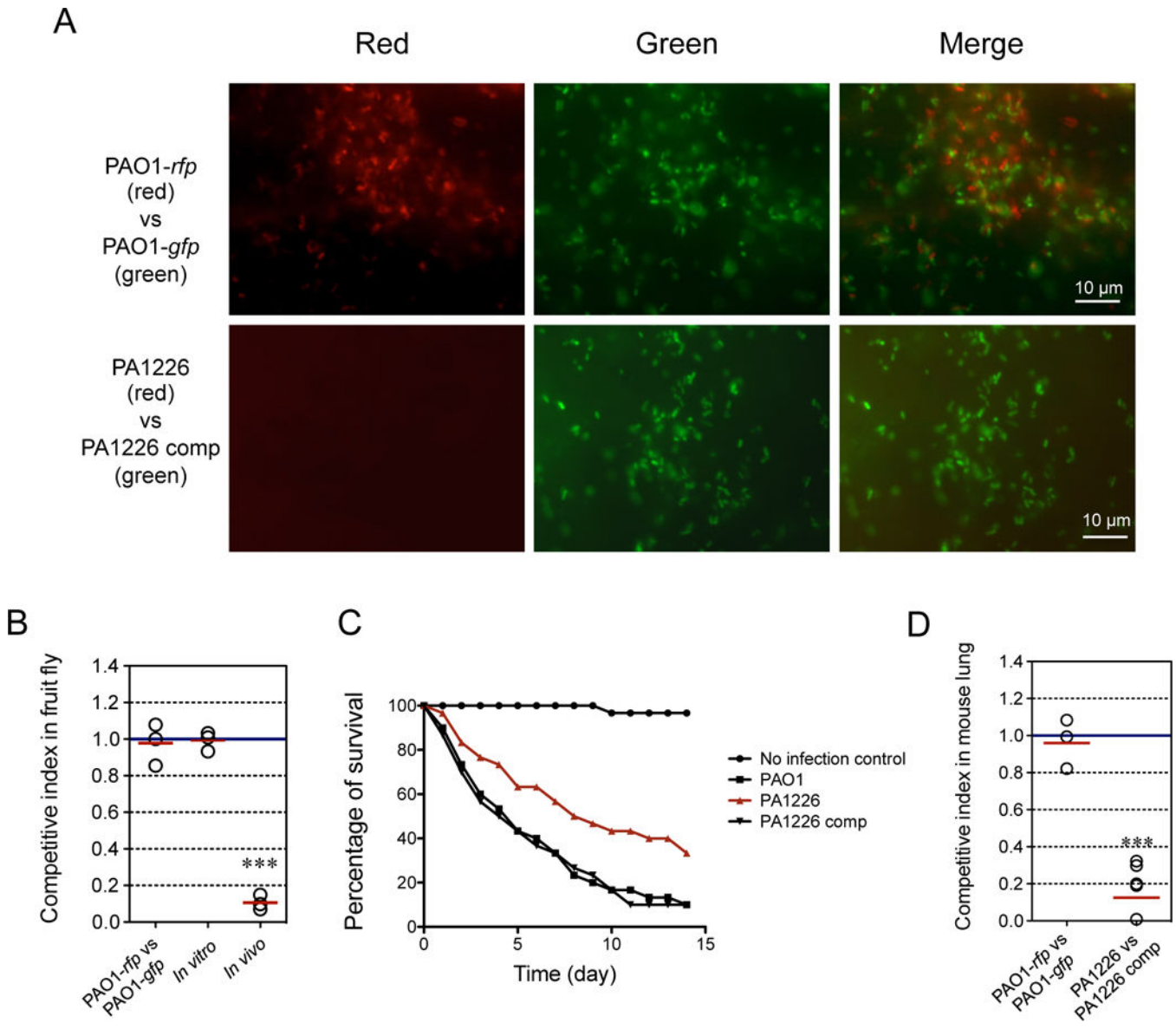

Figure 2.

Contribution of PA1226 to virulence in fruit fly and mouse lung infection models. (A) *In vivo* competition between the mutant strain (tetracycline resistant and RFP-tagged) and its corresponding complemented strain (gentamycin resistant and GFP-tagged). Control experiment was performed using two strains of wild-type PAO1 tagged with either tetracycline resistance and RFP marker, or gentamycin resistance and GFP marker. Crops were harvested from infected flies 48 h post infection and microscopic images showing PA1226 mutant was out-competed by the PA1226 complemented strain because there was a lack of red PA1226 mutant bacteria, while control experiment showed equal amount of RFP and GFP bacteria. (B) Competitive index of bacteria harvested from whole infected flies confirmed the microscopic results showing PA1226 mutant has reduced ability to colonize in fruit flies. The solid red line represents the average competitive index (CI) in each competition group. CI < 1 indicates that the mutant was out-competed by its complemented

strain in fruit flies (***, $P < 0.0005$). The PAO1-*rfp* vs PAO1-*gfp* control was performed the same as in (A) indicating no competitive difference between PAO1-*rfp* and PAO1-*gfp* strains. Additional control of *in vitro* CI was included by culturing the PA1226 mutant and complemented strains in 1:1 ratio in LB medium and no competitive difference is observed. (C) Survivals of flies infected by different *P. aeruginosa* strains were monitored compared to no bacteria control. Mutation in PA1226 decreased the level of virulence in fruit flies. (D) PA1266 mutant exhibited similar competitive disadvantage against the complemented strain in mouse lung infection model (**, $P < 0.005$; ***, $P < 0.0005$). As controls, three mice were inoculated with 1:1 mixture of two PAO1 strains tagged with tetracycline and gentamycin resistance markers, respectively, showing no difference in fitness.

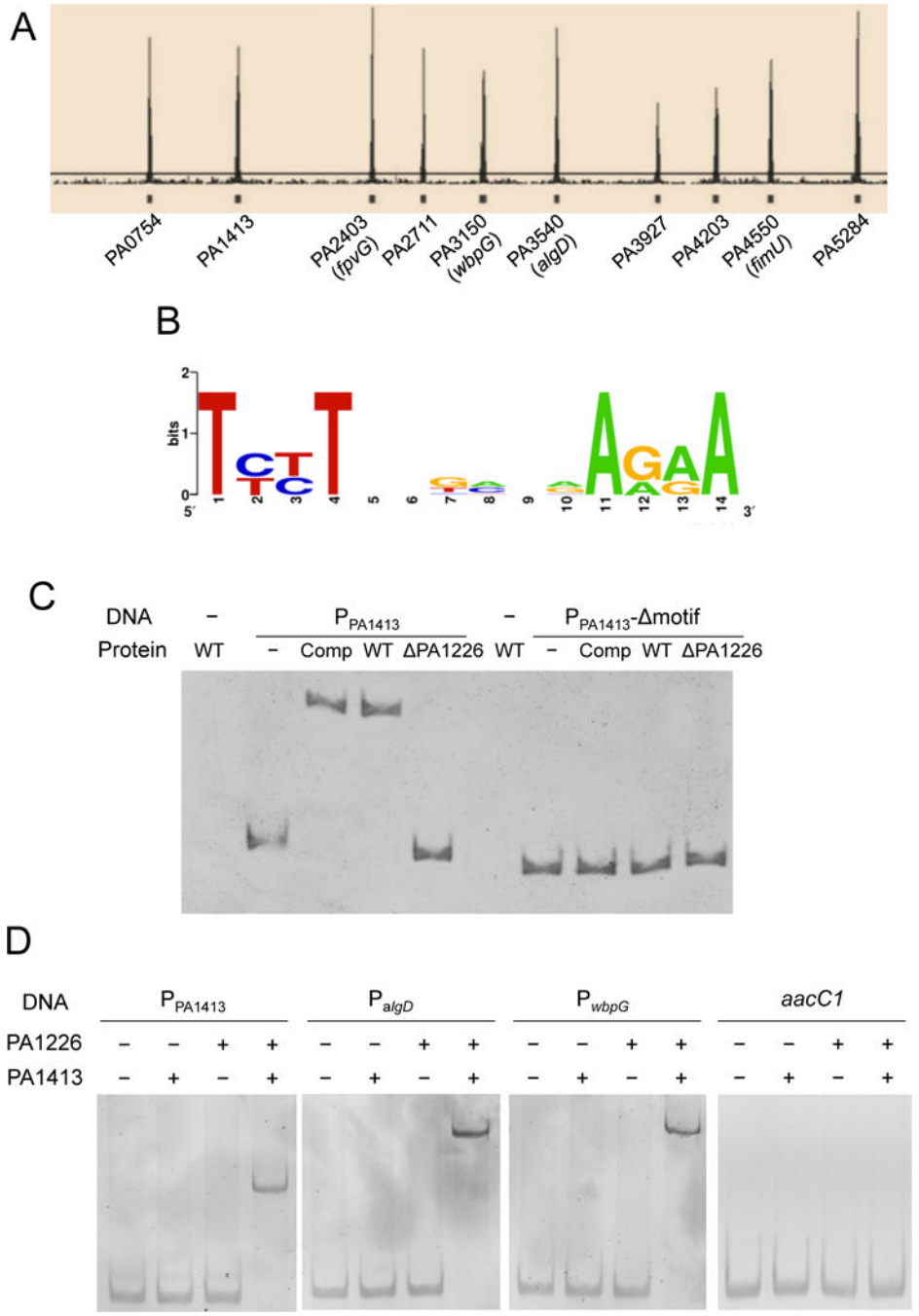

Figure 3.

The regulatory role of PA1226. (A) Mapped peaks from ChIP-seq results. PA# indicate predicted genes controlled directly by PA1226. (B) Binding motifs were predicted using online software CompleteMOTIFs. (C) EMSA with *P. aeruginosa* whole cell lysates and promoter region of PA1413 as an example. Binding was only detected using lysates with intact PA1226 (PAO1 and PA1226 complemented strains) and DNA fragments containing the motif. (D) EMSA with purified regulator PA1226 and co-regulator PA1413. His_6-tagged recombinant regulatory proteins His_6-PA1226 and His_6-PA1413 completely shifted

promoter regions of PA1413, *algD,* and *wbpG*. No shift was observed when PA1226 and PA1413 were used alone. An additional negative control using a DNA fragment of gentamycin resistance gene *aacC1* confirmed that the interaction were specific between PA1226+PA1413 and promoter regions of PA1413, *algD,* and *wbpG.*

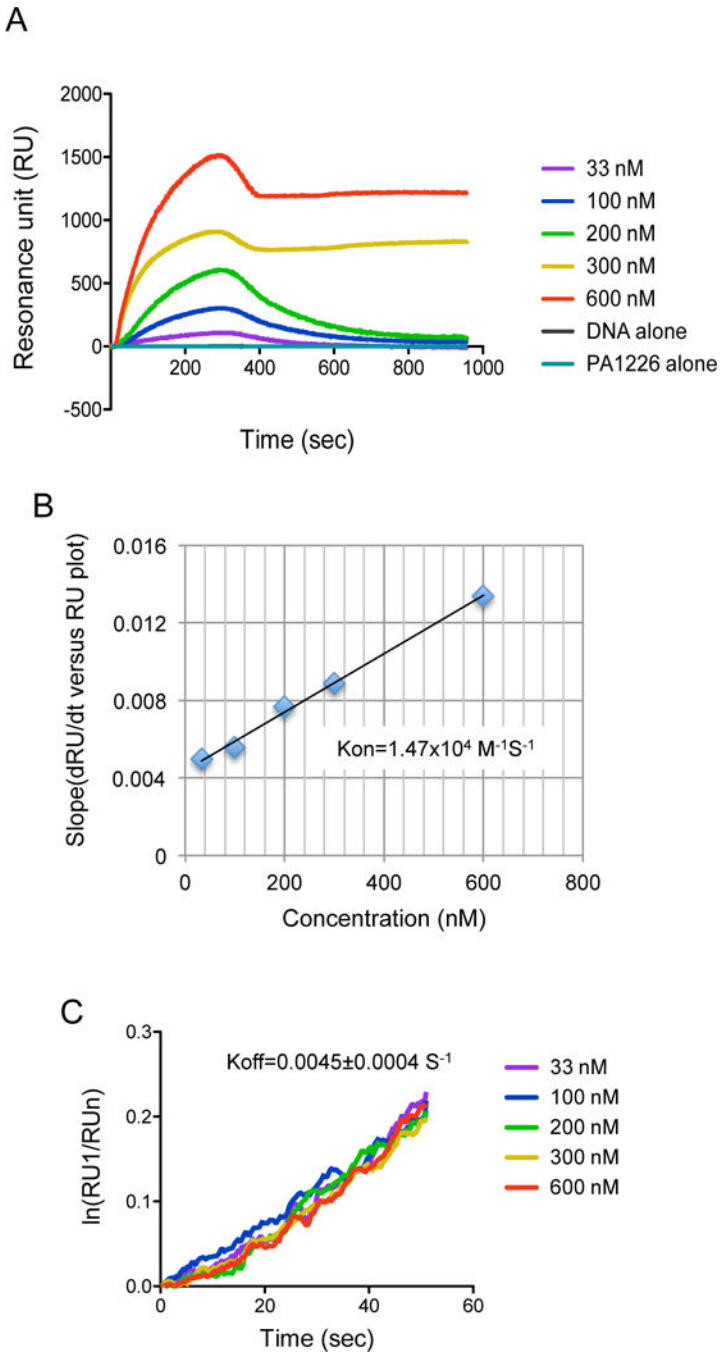

Figure 4.

Determination of the kinetic parameters (on-rate and off-rate) of the interaction between PA1413, PA1226, and DNA complex. His_6-PA1413 was covalently immobilized to an NTA sensor. Untagged PA1226 and DNA containing binding sequences functioned as analytes. (A) Sensorgram data plotted on dRU/dt versus RU plot. (B) Linearized data from sensorgrams for the determination of the on-rate (slope of the plot). (C) Linearized data from sensorgrams for the determination of off-rate (slope of the plot).

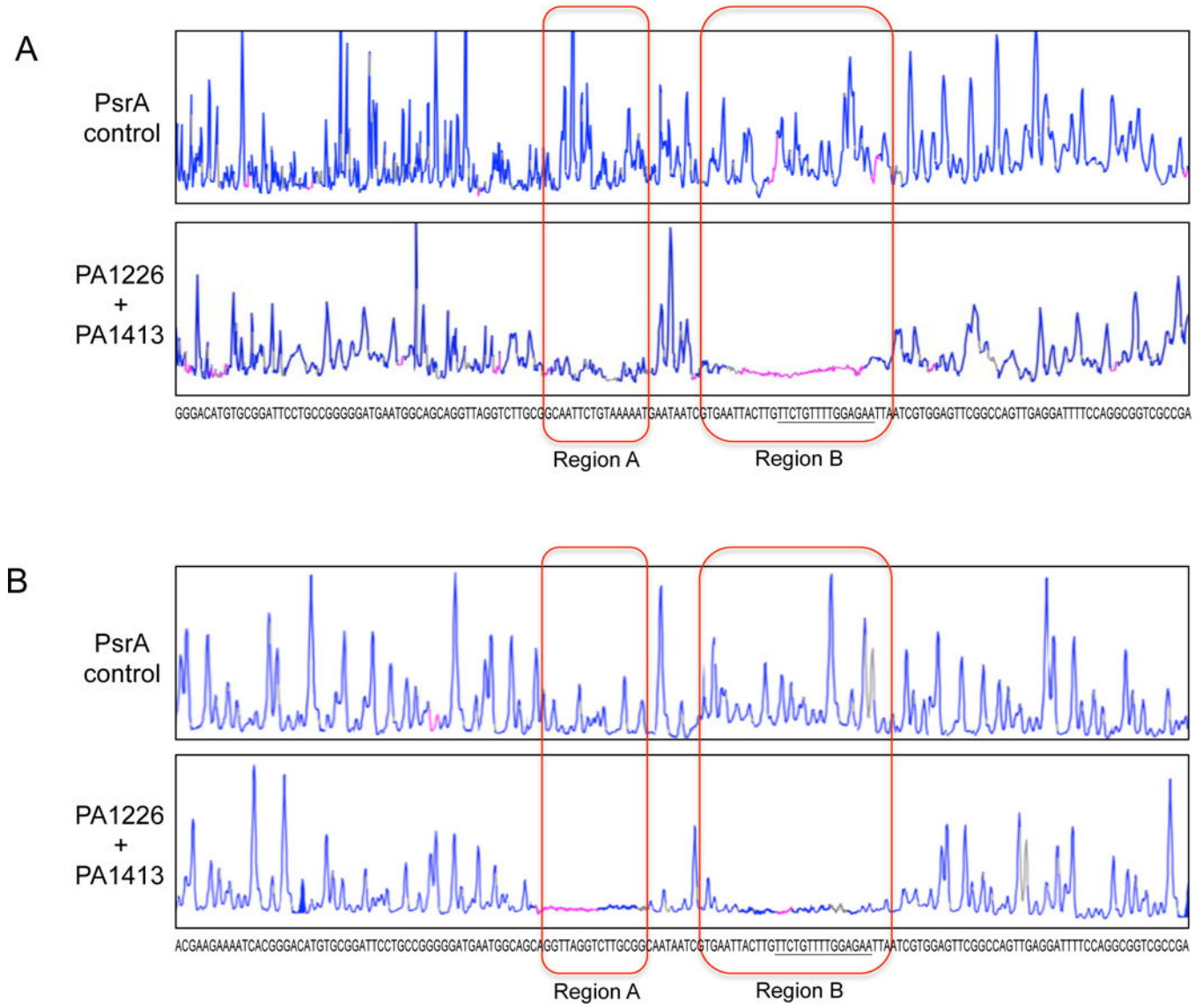

Figure 5.

Binding region of PA1226 and PA1413 observed via DNA Footprinting. (A) Trace shown in the upper panel was done with a regulator PsrA that does not bind to and protect promoter region of PA1413 as negative control; and the PA1226+PA1413 protected DNA trace is shown in the lower panel. The boxed regions are the predicted DNA binding sequence of PA1226+PA1413. The DNA fragment protected from DNase I digestion is consisted of region A (16 bp) and region B (30 bp), separated by a 8 bp sequence not protected by PA1226+PA1413. The 15 bp binding motif identified via ChIP-seq (underlined) is contained within region B. (B) DNA footprinting was repeated using promoter fragment with the 16 bp (GCAATTCTGTAAAAAT) in region A deleted. A different 16 bp sequence is now protected from DNase I digestion, suggesting that this region A is not sequence specific.

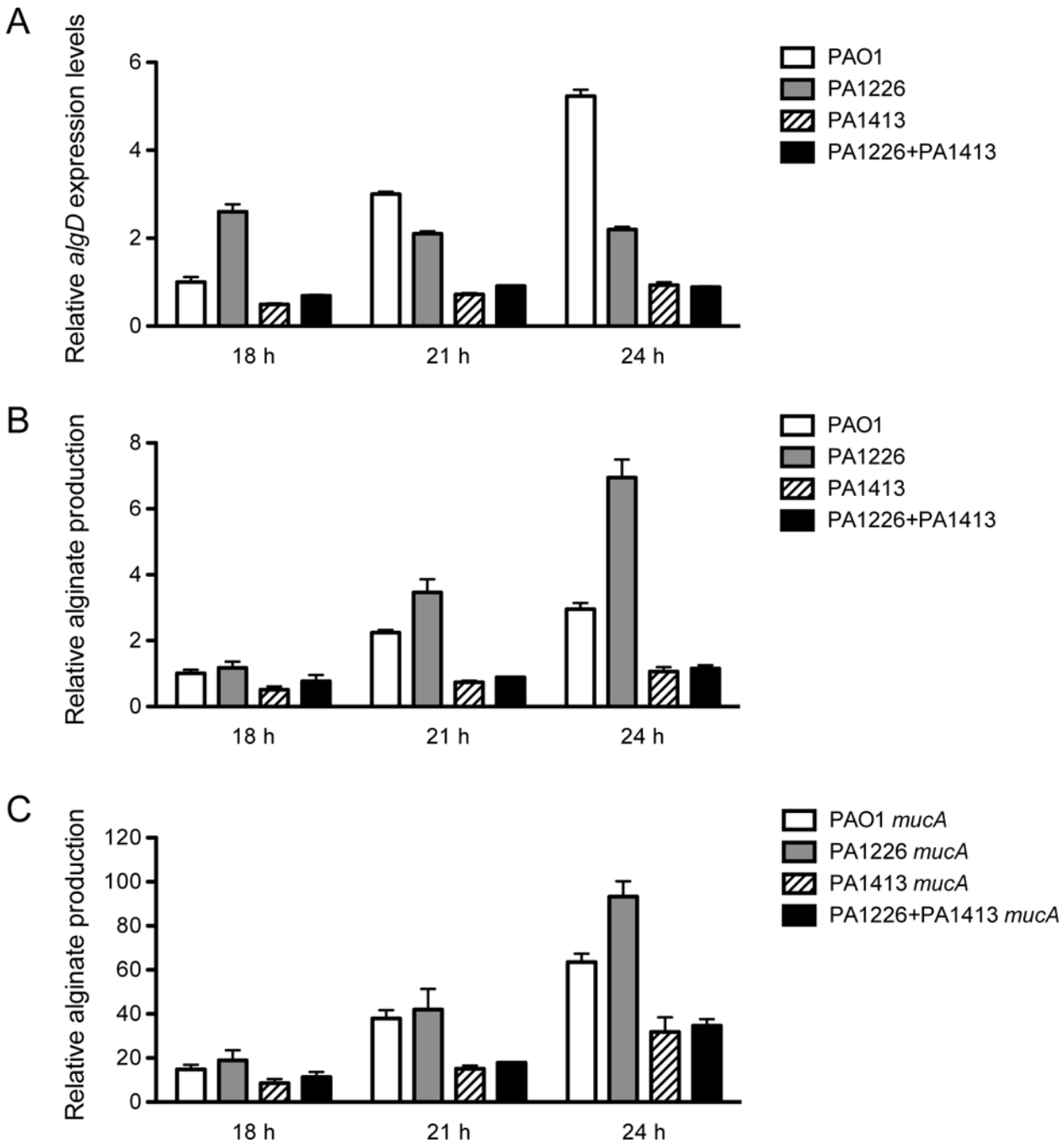

Figure 6.

Expression of *algD* and extracellular alginate production. (A) Relative expression levels of *algD* gene in PAO1 and various mutant strains; (B) Amount of extracellular alginate produced by PAO1 and various mutant strains. (C) Amount of extracellular alginate produced in same strains as (B) with additional *mucA* mutation, showing the regulation of alginate production by PA1226 and PA1413 is independent of *mucA*. Alginate levels in all strains were normalized to wild-type PAO1 strain.

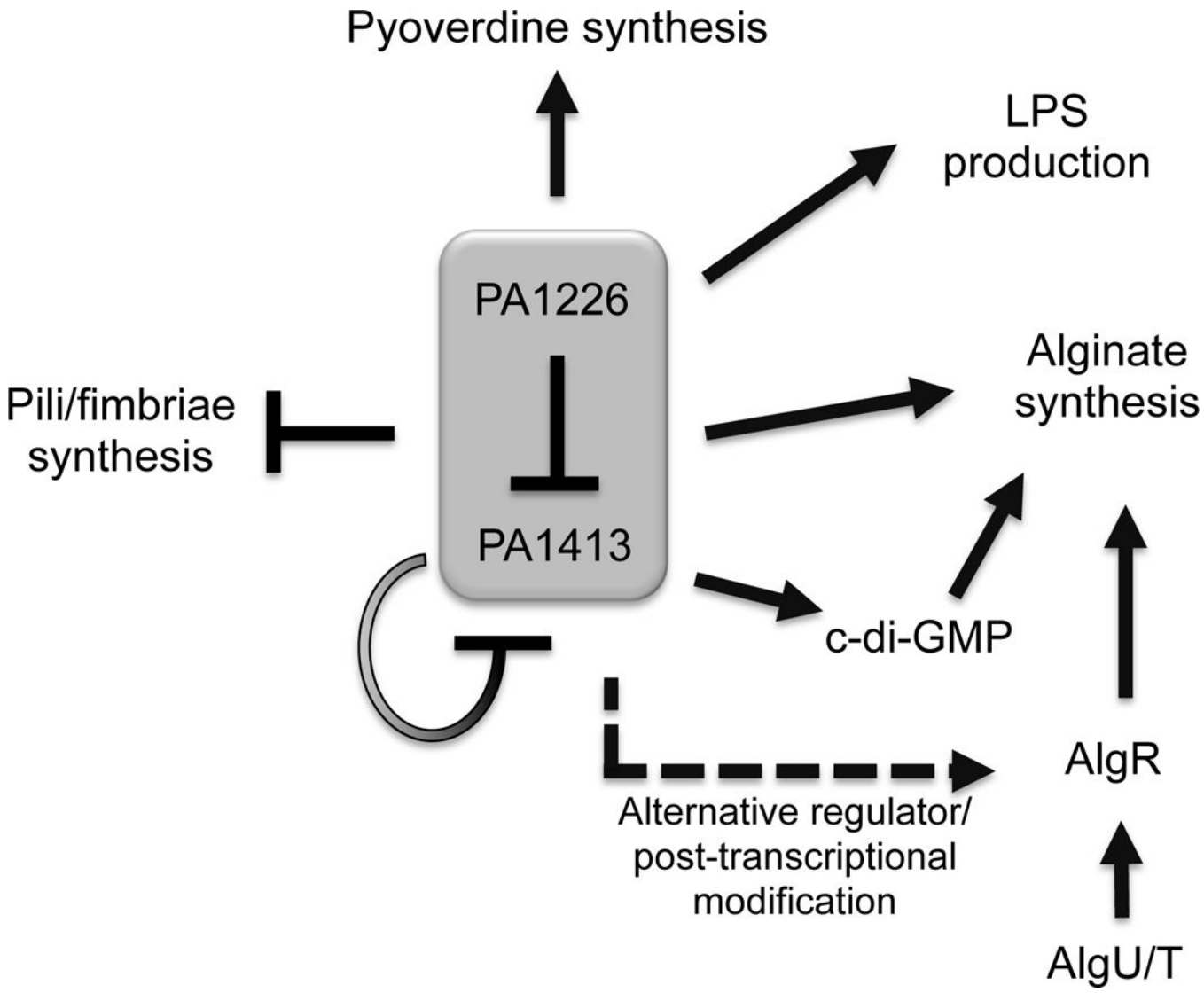

Figure 7.

Working model of the regulation of pili, LPS, and alginate production by PA1226-PA1413 dual-regulator system. The dual-regulator PA1226-PA1413 inhibits the expression of PA1413 and biosynthesis of pili/fimbriae, while activating the production of pyoverdine, LPS, and alginate. PA1226-PA1413 down-regulates pili/fimbriae biosynthesis and up-regulates pyoverdine and LPS production through directly interacting with their respective promoter regions. Its modulation on alginate production is achieved by direct binding to *alg*-operon promoter region, as well as a possibly indirect effect through c-di-GMP, a growth phase dependent modulation and/or post-translational modification.

Table 1.

P. aeruginosa genes and operons directly regulated by PA1226.

Gene ID	Gene Name/Function	Activated or repressed by PA1226
PA0754	Hypothetical protein	Repressed
PA1413	Probable transcriptional regulator	Repressed
PA2403-PA2406	FpvGHJK, pyoverdine biosynthesis	Activated
PA2711	Hypothetical protein	Repressed
PA3150-PA3148	WbpGHI, LPS biosynthesis	Activated
PA3540-PA3548	AlgD-AlgI, alginate biosynthesis	Activated
PA3927	Probable transcriptional regulator	Activated
PA4203	Probable transcriptional regulator	Repressed
PA4550-PA4556	FimU-PilVWX, type 4 fimbrial biogenesis	Repressed
PA5284	Hypothetical protein	Activated